ORIGINAL RESEARCH

Circular RNA Pum_0014 Targets miR-146a-5p/NF2 Axis to Regulate VEGF/PAK1 Pathway and Reduce H2O2-induced Cardiomyocyte Apoptosis

Yu Tang, PhD; Yun-Xia Wang, PhD; Yu-Liang Zhan, PhD; Yan-Feng Liu, PhD; Gui-Ping Wu, MS; Li-Dan Wen, MS

ABSTRACT

Circular RNAs (circRNAs) have emerged as essential regulators in cardiovascular disease, including acute myocardial infarction (AMI). This study investigated the role of circRNA Pum1_0014 in myocardial infarction (MI) and its underlying mechanisms using an H9C2 cell model. Through Sanger sequencing, nucleic acid electrophoresis, RNase R, and transcriptional inhibition experiments, Pum1_0014 was identified as a novel circRNA. The cell localization of circRNA Pum1_0014 was detected by qPCR and fluorescence in situ hybridization, and the results revealed that circRNA Pum1_0014 is predominantly located in the cytoplasm. StarBase (URL: http://starbase.sysu.edu.cn/) and TargetScan (URL: https://www.targetscan.org/vert_80/) were used to predict circRNA Pum1_0014 targeting miRNAs and miRNA targeting mRNA, and the results identified miR-146a-5p as a potential target of Pum1_0014, which in turn targets NF2. The plasmid encoding the mutant circRNA Pum1_0014 or the 3'UTR mutant NF2 was constructed, and the interaction between Pum1_0014 and miR-146a-5p or miR-146a-5p and NF2 was detected by luciferase reporter gene assay. The results confirmed the interactions between Pum1_0014, miR-146a-5p, and NF2. In the MI cell model, upregulation of circRNA Pum1_0014 and NF2 and downregulation of miR-146a-5p were observed. Knockdown of circRNA Pum1_0014 inhibited NF2 expression and activated the VEGF/PAK1 pathway, reducing cardiomyocyte apoptosis. Conversely, inhibition of miR-146a-5p and overexpression of NF2 had opposite effects. These findings suggest that circRNA Pum1_0014 acts through the miR-146a-5p/NF2 axis to reduce cardiomyocyte apoptosis in MI via the VEGF/PAK1/NF2 pathway. (*Altern Ther Health Med.* [E-pub ahead of print.])

Yu Tang, PhD; **Yun-Xia Wang, PhD**; **Yu-Liang Zhan, PhD**; **Yan-Feng Liu, PhD**, Department of Cardiology; Jiangxi Provincial People's Hospital; Nanchang; China. **Gui-Ping Wu, MS**, Department of Cardiology; Medical College of Nanchang University; Nanchang; China. **Li-Dan Wen, MS**, Clinical Research Institute; Jiangxi Provincial People's Hospital; Nanchang; China.

Corresponding author: Yu Tang, PhD
E-mail: yutangdoctor@126.com

INTRODUCTION

Acute myocardial infarction (AMI), the most severe type of coronary artery disease, is a prime reason for death.[1] More than 800 000 people experience myocardial infarction (MI) every year, and 27% die.[2] Recently, AMI has shown a trend toward younger age.[3] Therefore, AMI is becoming a significant health problem worldwide. Although clinical AMI treatment strategies have improved in recent years, patients remain unsatisfied.[4] Cardiomyocyte apoptosis was accepted as the primary mode of cell death after MI.[5] Therefore, inhibiting cardiomyocyte apoptosis may be a potential therapeutic strategy for treating MI.

Circular RNAs (circRNAs) are a newly discovered class of endogenous non-coding RNAs exhibiting high eukaryotic transcriptome expression levels.[6] Unlike linear RNAs, circRNAs possess a covalently closed circular structure, which confers resistance to degradation by nucleases due to the absence of a 5'-end cap structure and a polyadenylic acid structure at the 3' end.[7,8] Recently, the critical role of circRNAs in cardiovascular disease has been increasingly concerned.[9] Some studies reported that circRNA Nfix induces post-MI cardiac regeneration.[10] CircHipk3 works as a microRNA (miR)-133a sponge to enhance connective tissue growth factor expression, and circMACF1 attenuates AMI through the miR-500b-5p-EMP1 axis.[11,12] CircZNF609 plays a regulatory role in pulmonary fibrosis by acting through the miR-145-5p/KLF4 axis and influencing its translation function.[13] circMAML3 was reported to promote tumor progression of prostate cancer by regulating miR-665/MAPK8IP2 axis.[14] Thus, these studies illustrate that circRNAs may be a significant potential therapeutic target in MI.

Identifying and characterizing circRNAs have opened up new avenues for understanding the regulatory mechanisms underlying cardiovascular diseases, including MI.[15] Given

the unique stability and regulatory functions of circRNAs, they represent attractive targets for therapeutic interventions. The potential of circRNAs to modulate critical molecular pathways involved in MI pathogenesis provides a strong rationale for further investigation into their roles and therapeutic potential.

This study aims to explore the functional significance of circRNA Pum1_0014 in MI. By investigating its interaction with miR-146a-5p and its downstream target NF2, as well as its impact on the VEGF/PAK1 pathway, we seek to elucidate the underlying mechanisms by which circRNA Pum1_0014 regulates cardiomyocyte apoptosis in the context of MI. Understanding the role of circRNA Pum1_0014 in MI pathophysiology may contribute to developing novel therapeutic strategies for treating this devastating cardiovascular condition.

METHODS

Cell culture

H9C2 cells obtained from Xiamen Immocell Biotech were cultured in Dulbecco's modified Eagle's medium (catalog number: 11965084, Gibco, USA) where 10% fetal bovine serum (catalog number: 10099141C, Gibco, USA), four mM glutamine, and 100 U/ml penicillin-streptomycin (catalog number: 15070063, Gibco, USA) were added, and maintained in a 37°C/5% CO_2 incubator. H9C2 cells were induced by 100 μM H_2O_2 (catalog number: H1009, Sigma-Aldrich, USA) for 6 hours as a model group. H9C2 cells served as the control group.

Sanger sequencing (SS), nucleic acid electrophoresis, and RNase R digestion

For SS, PCR amplification products separated from agarose gel were purified, followed by SS determination of nucleotide sequences of the purified fragments using the standard method. For RNase R digestion, 2 μg total RNA was extracted for 20 min with 3 U/μg RNase R (catalog number: R7092M, Beyotime, China) at 37°C. Pum1_0014 expressions were normalized against GAPDH. For nucleic acid, electrophoresis was performed by adding the PCR products amplified from complementary (cDNA) or genomic DNA (gDNA) templates to a nucleic acid dye GelRed (catalog number: GR501-01, Vazyme, Nanjing, Jiangsu, China)-containing 6× loading buffer. Following isolation by agarose gel electrophoresis (2%), the DNA fragments were imaged by UV transillumination.

Transcriptional inhibition assay with actinomycin D

H9C2 cells (500,000) planted in six-well plates for 12 h were immersed in an actinomycin D (2 μg/ml; catalog number: SBR00013, Sigma-Aldrich, USA)-supplemented fresh medium. Quantitative PCR (qPCR) analysis of total RNA extracted at 0, 8, 16, and 24 h after actinomycin D treatment was carried out.

Isolating H9C2 nucleus and cytoplasm

The H9C2 nucleus and cytoplasm were isolated using Nuclear and cytoplasmic extraction reagents (Catalog number: 78833, Thermo Scientific, USA). After separation, Pum1_0014, U6, and 18S rRNA expressions were quantified using qPCR, which served as references for nuclear and cytoplasmic RNA, respectively.

Fluorescence in situ hybridization (FISH)

The subcellular localization of circRNA Pum1_0014 was investigated by RNA-FISH. Cy3-labeled circRNA Pum1_0014, U6, and 18 rRNA probes were supplied by RIBOBIO (Guangzhou, China). Fluorescence signals were generated using a Fluorescent In Situ Hybridization Kit (Catalog number: C10910, RiboBio, China). A Zeiss LSM980 + Airyscan2 machine was employed to capture images.

Bioinformatic analysis

StarBase (URL: http://starbase.sysu.edu.cn/) and TargetScan (URL: https://www.targetscan.org/vert_80/) were utilized for the prediction of the potential miRNA-binding targets of circRNA Pum1_0014 and the target mRNAs of miR-146a-5p, respectively.

Plasmid, mimic, and inhibitor

miR-146a-5p mimic and its negative control (mimic NC), miR-146a-5p inhibitor and its negative control (inhibitor NC), the plasmid encoding short hairpin RNA (shRNA) of circRNA Pum1_0014 (shPum1_0014), the plasmid encoding the negative control of shPum1_0014 (shNC), the plasmid encoding NF2 pcDNA-NF2, the plasmid encoding wild type Pum1_0014 (Pum1_0014 WT), the plasmid encoding mutant Pum1_0014 (Pum1_0014 MUT), the plasmid encoding wild type NF2 3'UTR (NF2 3'UTR WT), and the plasmid encoding mutant NF2 3'UTR (NF2 3'UTR MUT) were constructed by XIAMEN Anti-HeLa Biological Technology Trade Co. Ltd. Sequences of mimic, inhibitor, and primers for plasmid construction are list in table 1.

Table 1. Sequences of mimic, inhibitor, and primers for plasmid construction

Name	Sequence (5'-3')
miR-146a-5p mimic	UGAGAACUGAAUUCCAUGGGUU
mimic NC	UUGUACUACACAAAAGUACUG
miR-146a-5p inhibitor	AACCCAUGGAAUUCAGUUCUCA
inhibitor NC	CAGUACUUUUGUGUAGUACAA
shPum1_0014 F	CCGGCATCCCTTGGGCCCTGTTGTTCTCGAGAACAACAGGGCCCAAGGGATGTTTTT
shPum1_0014 R	AATTAAAAACATCCCTTGGGCCCTGTTGTTCTCGAGAACAACAGGGCCCAAGGGATG
shNC F	CCGGCATCCCTTGGGCCGACAACAACTCGAGTTGTTGTCGGCCCAAGGGATGTTTTT
shNC R	AATTAAAAACATCCCTTGGGCCGACAACAACTCGAGTTGTTGTCGGCCCAAGGGATG
Pum1_0014 WT F	AGCTCGCTAGCCTCGAGCTGTTGTTGAGAATTGTAG
Pum1_0014 WT R	CATGCCTGCAGGTCGACGGCCCAAGGGATGCAGACAG
Pum1_0014 MUT F	TCCTGTCCCTTGGCACCATTGGTGCTG
Pum1_0014 MUT R	AGGGACAGGAGGATTTCTCCAACATG
pcDNA-NF2 F	AGATTCTAGAGCTAGCGAATTCATGGCCGGAGCCATCGCTTC
pcDNA-NF2 R	TTCGCGGCCGCGGATCCTCAAATGCAGATAGGTCTTC
NF2 3'UTR WT F	ACGAGCTCGCTAGCCTCGAGCTTACTCTGCAGAGCG
NF2 3'UTR WT R	CATGCCTGCAGGTCGACCTTCTCAAACCAAAGTCAGC
NF2 3'UTR MUT F	TGTTCTAGTTCTCCTAGCCTGCATATCTATG
NF2 3'UTR MUT R	AGGCTAGGAGAACTAGAACACCTTGAGAAATC

Abbreviaitions: F, forward primer, R, reverse primer.

Cell Transfection

H9C2 cells planted in the wells of 6-well plates were subjected to transfection with 5 μg of plasmid (shPum1_0014, pcDNA-NF2, or/and their negative control), 200 pmol miRNA mimic, or 200 pmol miRNA inhibitor when they were 80% confluent following the Lipofectamine 2000 (Catalog number: 11668500, Invitrogen, USA) instructions. Cells were harvested 24 h later for subsequent assays.

Luciferase reporter gene assay

mimic NC and miR-146a-5p mimic were co-transfected with Pum1_0014 WT or MUT and NF2 3'UTR MUT or WT using Lipofectamine 2000 reagent into H9C2, and TK vector co-transfection was performed simultaneously. After lysis that was conducted at 24 h post-transfection, the luciferase activities (firefly and Renilla luciferase activities) were determined using a dual luciferase assay system (Catalog number: E2920, Promega, USA), with the former normalized against the latter to calculate the expression level.

qPCR

Total RNA was extracted from H9C2 using TRIZOL (Catalog number: 15596018CN, Invitrogen, USA) reagent. Using a PrimeScript RT Reagent Kit (Catalog number: RR047A, Takara, Japan), cDNA was collected via reverse transcription (RT) of high-quality total RNA. Then, the primers were employed to perform the PCR reaction with the Agilent-Strata gene MxReal-Time qPCR system and TB Green Premix Ex Taq II (Catalog number: RR82LR, Takara, Japan). Pum1_0014, NF2, VEGF, and PAK1 levels were normalized by 18S rRNA, whereas U6 calibrated miR-146a-5p expression because of its nuclear location. The primers for qPCR are listed in Table 2.

CCK-8 assay

After seeded at a density of 8000 cells per well in 96-well plates, H9C2 or H9C2 MI cells were transfected with relative plasmids for 24 hours. To assess cell viability, 10 μL CCK-8 solution was added to the cell culture medium. After a 2-hour culture at 37°C, the absorbance at optical density 450nm was detected by a microplate reader (Thermo Fisher Scientific, USA). Cell viability was calculated based on the OD value in the control group after normalization.

Annexin V- FITC/ PI assay

H9C2 cells at 48 h post-transfection were gathered for 20 min of staining using an annexin V-FITC/PI Apoptosis Detection kit (Catalog number: A211-01, Vazyme, Nanjing, Jiangsu, China), followed by flow cytometry analysis.

Western blotting

H9C2 cells were maintained in a phosphatase inhibitor-containing ice-cold RIPA buffer for 30 min. This was followed by homogenization and sonication. Proteins were extracted and quantified using a BCA kit (Catalog number: PA115-02; TIANGEN Biotechnology, Beijing, China) to determine concentration. After samples containing loading buffer boiled at 95°C for 10 min, 20 μg protein per well was blotted onto 10% SDS-PAGE gels. Following electrophoresis and transfer, the membranes were blocked with 5% skimmed milk for 1 h. After 3 times wash by PBST, the membrane was incubated with 1% TBST buffer containing VEGF (1:2000, Catalog number: 19003-1-AP), PAK1 (1:2000; Catalog number: 21401-1-AP), NF2 (1:2000; Catalog number: 21686-1-AP), and GAPDH (1:5000; Catalog number: 10494-1-AP) all purchased from Proteintech (China), respectively, for overnight at 4°C. After PBST was rinsed thrice, the membrane grew with a 1:10 000 diluted second antibody. After another three washes (3 × 10 min), the membrane was added with an ECL kit for protein band visualization using a Bio-Rad ChemicDoc machine. The relative protein expression levels of VEGF, PAK1, and NF2 were normalized against GAPDH.

Table 2. The primers for qPCR

Primer name	Sequence (5'-3')
GAPDH F	CGCTGAGTACGTCGTGGAGTC
GAPDH R	GCAGGAGGCATTGCTGATGA
Pum1_0014 F	CCTCCTTCAAATCTCCTA
Pum1_0014 R	ACTACAATTCTCAACAACA
U6 F	CTCGCTTCGGCAGCACA
U6 R	AACGCTTCACGAATTTGCGT
U6 RT	AACGCTTCACGAATTTGCGT
miR-146a-5p RT	GTCGTATCCAGTGCAGGGTCCGAGGTATTCGCACTGGATACGACAACCCA
miR-146a-5p F	CGCGTGAGAACTGAATTCCA
miR-146a-5p R	AGTGCAGGGTCCGAGGTATT
18S rRNA F	AGGCGCGCAAATTACCCAATCC
18S rRNA R	GCCCTCCAATTGTTCCTCGTTAAG
NF2 F	TGAACGCACGAGGGATGAGTTG
NF2 R	GCCTTTTCAGCCAACAGGTCAG
PAK1 F	GTGAAGGCTGTGTCTGAGACTC
PAK1 R	GGAAGTGGTTCAATCACAGACCG
VEGF F	TTGCCTTGCTGCTCTACCTCCA
VEGF R	GATGGCAGTAGCTGCGCTGATA

Abbreviaitions: F, forward primer, R, reverse primer.

Statistical analyses

GraphPad Prism v 8.0 was employed for statistical analyses. One-way analysis of variance (ANOVA) followed by Tukey's post-hoc test was adopted for multi-group comparisons. At the same time, the student's *t*-test (unpaired) was applied to between-group comparisons of parametric data. For calculating the relative mRNA expression of the gene of interest, the formula for estimating the relative mRNA expression of the gene of interest is Expression of the gene of interest = C(T) value of gene of interest / C(T) value of internal control gene. This approach allows normalizing gene expression levels and comparing samples or experimental conditions. Western blotting was performed by scanning, and the signal intensity was quantified using ImageJ software.[16]

RESULTS

Pum1 0014 is identified as a circRNA

We investigated whether Pum1_0014 functions as a circRNA. First-generation sequencing (Figure 1A) and nucleic acid electrophoresis of Pum1_0014 and GAPDH (Figure 1B) were used to figure out the structure of Pum1_0014. As an exoribonuclease, RNase R digests almost

Figure 1. Identified Pum1_0014 as a novel circRNA. **A.** Generation Sequencing Analysis of sequences of Pum1_0014. **B.** Divergent primers amplify circRNA Pum1_0014 in cDNA but not genomic DNA (gDNA); the arrow direction indicates divergent and convergent primers. **C.** RNase tolerance experiment. GAPDH and Pum1_0014 levels were detected after treatment with or without RNase R. **D.** Transcriptional inhibition experiments. H9C2 cells were treated with 1 μM Actinomycin D (Sigma) for 0, 8, 16, or 24 hours respectively. Total RNA was extracted and for qPCR quantification of Pum1_0014 and GAPDH expression. Pum1-0014: circRNA Pum1_0014, bp: base pair. * $P < .05$, *** $P < .001$, **** $P < .0001$, ns means $P > .05$.

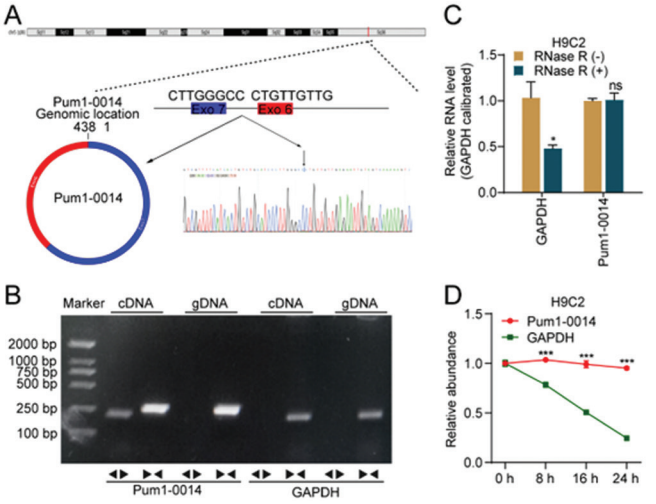

all linear RNA but not circRNA. As shown in Figure 1C, the expression of Pum1_0014 did not change after treatment with RNase R. Additionally, when compared with GAPDH, the expression of Pum1_0014 did not decrease after treatment with the transcriptional inhibitor actinomycin D for different times (Figure 1D). In summary, these results confirm that Pum1_0014 is a circRNA.

CircRNA Pum1_0014 located in cytoplasm

To understand the mechanism of circRNA Pum1_0014, its location was determined by nuclear separation and FISH experiments. H9C2 cells were collected, and the nucleus and cytoplasm were separated using nuclear and cytoplasmic extraction reagents (Catalog number: 78833, Thermo Scientific, USA). The enrichment of Pum1_0014 was the same as that of 18S, which was localized in the cytoplasm (Figure 2A). In addition, FISH experiments revealed that Pum1_0014 appeared in the cytoplasm but the nucleus (Figure 2B).

CircRNA Pum1_0014 functioned as a miR-146a-5p ceRNA to upregulate NF2

Online prediction tools (miRanda and starBase v2.0) were used to identify miR-146a-5p as a potential target to investigate Pum1_0014 interacting miRNAs (Figure 2C), which returned NF2 as a possible target of miR-146a-5p

Figure 2. Location of Pum1_0014 and Pum1_0014 targets with miR-146a-5p to regulate NF2. **A.** Nuclear separation experiment. The H9C2 nucleus and cytoplasm were separated using a Thermo kit, and Pum1_0014, 18S, and U6 expressions were detected, respectively. **B.** FISH experiment. Pum1_0014, 18S, and U6 probes were obtained from RIBOBIO company. **C-D.** Predicted targeting sites for Pum_0014 and miR-146a-5p by bioinformatics analysis. **E-F.** Dual luciferase reporter gene experiments showed the effect of miR-146a-5p with Pum1_0014 and NF2. **G-I.** Pum1_0014 and NF2 expression were detected after overexpressing miR-146-5p in H9C2. **J.** Cytotoxicity test of 100 μM hydrogen peroxide in H9C2 cells to assess the suitable treatment time for the myocardial infarction cell model. Pum1-0014: circRNA Pum1_0014. WT: wild type. Mut: mutant. ** $P < .01$, *** $P < .001$, **** $P < .0001$, ns means $P > .05$.

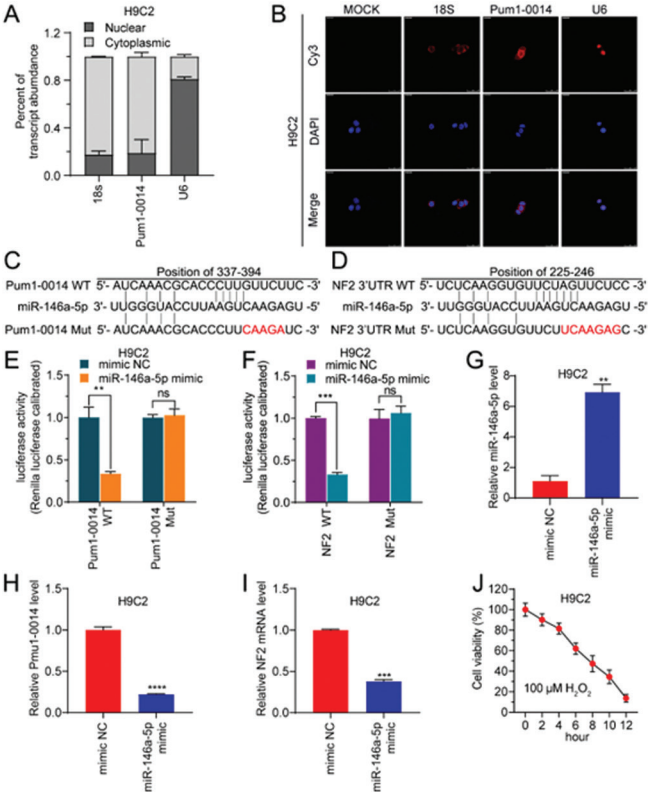

(Figure 2D). To validate the predicted targets of Pum1_0014 and miR-146a-5p, luciferase reporter gene assay was carried out on Pum1_0014 WT or MUT luciferase reporter plasmid-transfected H9C2. The luciferase activity was found to be reduced by miR-146a-5p mimics in Pum1_0014 WT cells but not significantly altered in Pum1_0014 MUT cells (Figure 2E). To validate the predicted miR-146a-5p and NF2 interactions, a luciferase reporter gene assay was performed on NF2 WT or NF2 MUT luciferase reporter plasmid-transfected H9C2. This result showed that miR-146a-5p mimics decreased luciferase activity in H9C2 cells transfected with the NF2 WT plasmid but not the NF2 MUT plasmid (Figure 2F). Besides, miR-146a-5p was up-regulated in miR-146a-5p mimic-transfected H9C2 ($P < .05$), indicating

Figure 3. Knockdowning Pum1_0014 and overexpressing miR-146a-5p reduce cardiomyocyte apoptosis in myocardial infarction. **A.** The mRNA level of Pum1_0014, miR-146a-5p, PAK1, VEGF, and NF2 were detected in diverse groups with or without knockdown of Pum1_0014 and overexpression of miR-146-5p in H9C2 cells. **B-C.** The protein levels of PAK1, VEGF, and NF2 were detected in diverse groups with or without knockdown of Pum1_0014 and overexpression of miR-146-5p in H9C2. **D.** Cell viability of diverse groups with or without knockdown of Pum1_0014 and overexpression of miR-146-5p in H9C2 cells by CCK8 assay. **E-F.** Apoptosis rates in diverse groups were detected by flow cytometry using Annexin V/PI assay. Pum1-0014: circRNA Pum1_0014. ** $P < .01$, *** $P < .001$, **** $P < .0001$

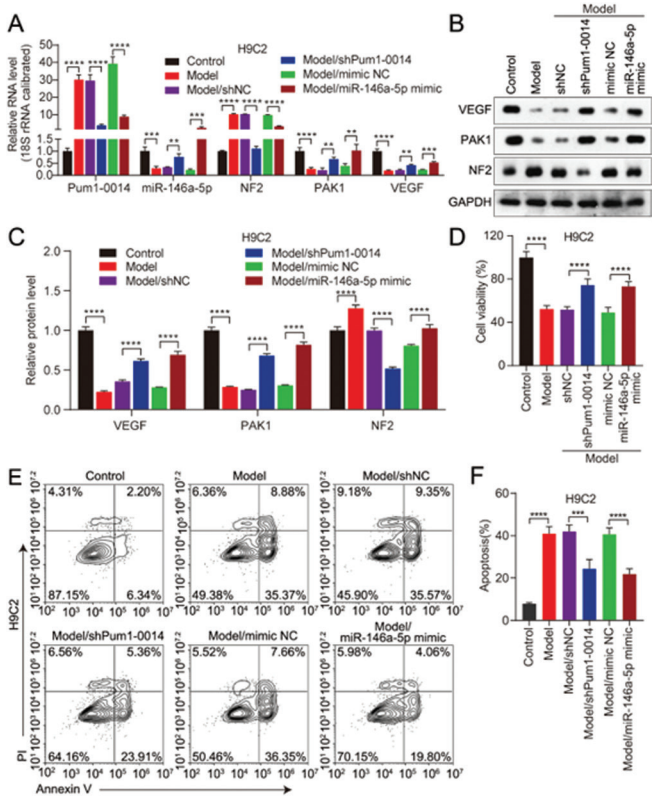

successful transfection (Figure2G). The expression levels of circRNA Pum1_0014 (Figure 2H) and NF2 mRNA (Figure 2I) significantly decreased in the miR-146a-5p mimic group. Hence, circRNA Pum1_0014 may upregulate NF2 expression through spongiform miR-146a-5p.

circRNA Pum1_0014 knockdown targets miR-146a-5p to reduce apoptosis through VEGF/PAK1/NF2 pathway

To investigate the function of circRNA Pum1_0014 in AMI, hydrogen peroxide was used to treat H9C2 cells to build the model (Figure 2J). After treatment with 100 μM H_2O_2 for 6 h, the cell viability was approximately 60%, considered the model-induced treatment. CircRNA Pum1_0014 and NF2 expression were upregulated in the MI model, whereas miR-146a-5p was downregulated versus the control group (Figure 3A-C). Thus, we performed Pum1_0014

Figure 4. Increased cardiomyocyte viability by knocking down Pum1_0014 and overexpressing miR-146a-5p were reversed by miR-146a-5p inhibitor and NF2 overexpression, respectively. **A.** miR-146a-5p inhibitor or NF2 overexpression reversed Pum1_0014, miR-146-5p, PAK1, VEGF, and NF2 levels in Pum1_0014-knockdown and miR-146a-5p-overexpressing H9C2 myocardial injury cell model cells, respectively. **B-C.** miR-146a-5p inhibitor or NF2 overexpression reversed PAK1, VEGF, and NF2 protein levels in Pum1_0014-knockdown and miR-146a-5p-overexpressing H9C2 myocardial injury cell model cells, respectively. **D.** Cell viability was reversed by miR-146a-5p inhibitor or NF2 overexpression after Pum1_0014 knockdown or miR-146a-5p overexpression in H9C2, respectively. Pum1-0014: circRNA Pum1_0014. *, **, ***, and **** indicate $P < .05$, $P < .01$, $P < .001$, and $P < .0001$, while ns means $P > .05$, respectively.

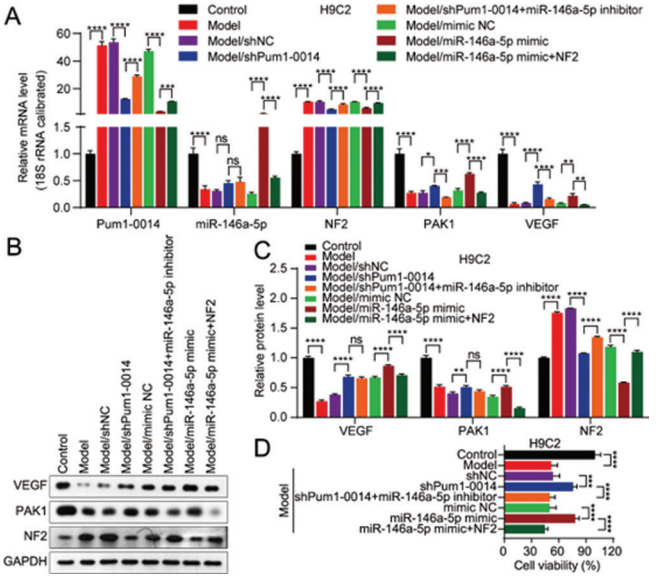

knockdown and miR-146a-5p overexpression using shRNA plasmid and miR-146a-5p mimics in the MI cell model, respectively (Figure 3A-C). Knockdown of Pum1_0014 upregulated miR-146a-5p and inhibited NF2 mRNA expression, while miR-146a-5p overexpression reduced Pum1_0014 and NF2 expression (Figure 3A-C). NF2-deficient mice have been reported to exhibit increased vascular structure and high bone marrow VEGF production.[17] Studies have shown that VEGF can be combined with erythropoietin to treat MI in ovine.[18] Taken together, these results suggest that reduced cardiomyocyte apoptosis by Pum1_0014 knockdown may be due to the activation of VEGF signaling. Next, we validated the expression of VEGF and PAK1 in an MI model. We found upregulated VEGF and PAK1 mRNA and protein expression by circRNA Pum1_0014 knockdown or miR-146a-5p overexpression (Figure 3A-C), consistent with the reported function of VEGF in MI. Cell viability increased in the Pum1_0014 knockdown and miR-146a-5p overexpression groups (Figure 3D). Consistent with this result, reduced apoptosis was observed in the Pum1_0014

Figure 5. Reduced cardiomyocyte apoptosis by knocking down Pum1_0014 and overexpressing miR-146a-5p were reversed by miR-146a-5p inhibitor and NF2 overexpression, respectively. **A-B.** miR-146a-5p inhibitor or NF2 overexpression reversed apoptosis rate in Pum1_0014-knockdown and miR-146a-5p-overexpressing H9C2 myocardial injury cell model cells, respectively. Pum1-0014: circRNA Pum1_0014. ***, and **** indicate $P < .001$, and $P < .0001$, respectively.

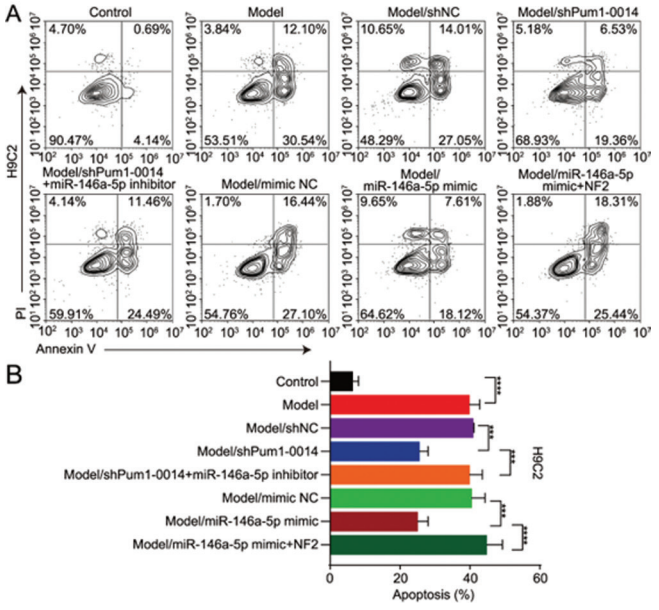

knockdown group and miR-146a-5p overexpression group (Figure 3E, F). To further understand the critical roles of circRNA Pum1_0014 in MI, co-transfection of the miR-146a-5p inhibitor and shPum1_0014, miR-146a-5p mimics and NF2 overexpression were performed, respectively (Figure 4A), which showed its successful transfection. Upregulated miR-146a-5p and decreased NF2 mRNA expression by knocking down Pum1_0014 or overexpressing miR-146a-5p were found to be reversed by miR-146a-5p inhibitor and NF2 overexpression, respectively (Figure 4A). Increased mRNA and protein levels of PAK1 and VEGF were also changed (Figure 4A-C). In addition, after transfection with the NF2 plasmid or miR-146a-5p, elevated cell viability and reduced apoptosis in Pum1_0014 knocked-down cells or miR-146a-5p-overexpressing cells were observed to be significantly decreased and increased, respectively (Figure 4D, 5A-B). These results indicated that the knockdown of circRNA Pum1 0014 reduced cardiomyocyte apoptosis via the miR-146a/NF2 axis. When NF2 expression is downregulated, the VEGF/PAK1 pathway is enhanced, thereby reducing apoptosis in MI.

DISCUSSION

CircRNAs, originally identified as the byproduct of aberrant splicing, were increasingly discovered as the high-throughput RNA-seq technique developed, allowing for the study of a wide range of biological functions of circRNAs.[15] Heart tissue detection using a deep sequencing approach revealed an abundance of circRNAs expressed in the heart, implying the key role circRNAs play in disease development.[19] Research on circRNAs has focused on competing endogenous RNAs or target RNA decoys and miRNA sponges through binding to RNA binding proteins (RBPs). In addition, circRNA also functions as a protein scaffold, facilitating the contact and assembly of proteins such as circFoxo3. Many circRNAs are cytoplasmically located, where they can play a role in sponging miRNA.[20] In contrast, others exist in the nucleus, where they may target snRNA, thus enhancing their parental genes' RNA POI II transcription activity.[21] In MI mice, CDR1as, first reported as a functional circRNA in MI, was highly expressed compared to healthy mice.[22] Overexpression of CDR1as increases cardiac infarct size via miR-7/PARP/SP1. In contrast, low MICRA expression was found in MI patients with left ventricular dysfunction. MICRA may rely on the sponges of miR-150, which appear after patients develop acute MI.[23] These studies confirmed the diverse functions of circRNA in MI patients and provided us with a novel potential therapeutic approach for MI.

In this study, we aimed to investigate the role of circRNAs in myocardial infarction (MI). We began by using rat cardiomyocyte H9C2 cells to identify a novel circRNA, Pum1_0014, employing multiple methods. We determined that Pum1_0014 is predominantly in the cytoplasm through subcellular localization analysis. Using bioinformatics, we predicted potential miRNAs that Pum1_0014 could target. To validate the functional relevance, we conducted experiments confirming that Pum1_0014 acts as a sponge for miR-146a-5p, consequently leading to the downregulation of NF2. This downregulation, in turn, promotes the VEGF/PAK1 pathway, ultimately reducing cardiomyocyte apoptosis in vitro.

Previous research has extensively explored the role of miR-146a-5p in various cardiovascular diseases.[24-26] Notably, miR-146a-5p has been identified as a crucial apoptosis regulator by suppressing vascular endothelial growth factor (VEGF).[27] Moreover, miR-146a-5p has been implicated in the regulation of cardiac fibrosis by targeting tumor necrosis factor receptor-associated factor 6 (TRF6) and inhibiting FGF2.[28,29]

While the NF2 gene has been extensively studied in the context of cancer, its role in cardiovascular diseases, particularly cardiomyocyte apoptosis, remains largely unexplored. Additionally, studies have reported that VEGF-A can promote angiogenesis after MI by increasing reactive oxygen species (ROS) production and enhancing endoplasmic reticulum (ER) stress-mediated autophagy.[30] Therapeutic strategies involving VEGF expression enhancement, such as VEGF nanoparticles or circFndc3b overexpression, have shown promising results in post-MI neovascularization and fibrosis alleviation.[31,32]

Despite the significant findings regarding the relationship between circRNAs, miR-146a-5p, NF2, and the VEGF/PAK1 pathway, our study has certain limitations. Further experiments could provide a more comprehensive understanding of their roles. For instance, investigating the

changes in ROS generation following knockdown of Pum1_0014 would offer valuable insights, given the observed activation of VEGF. Additionally, validating the function of Pum1_0014 in an in vivo mouse model of MI would help elucidate its therapeutic effects.

In conclusion, our study highlights the regulatory role of circRNA Pum1_0014 in the miR-146a-5p/NF2 axis, leading to modulation of the VEGF/PAK1 pathway and the reduction of H2O2-induced cardiomyocyte apoptosis. The potential of Pum1_0014 as a therapeutic target for MI holds significant promise, although further investigations are warranted.

CONCLUSION

Pum1_0014 knockdown is myocardial protective by increasing cardiomyocyte viability and reducing cardiomyocyte apoptosis through the miR-146a-5p binding mechanism. Besides, Pum1_0014 works as a miRNA sponge to inhibit miR-146a-5p function and regulates NF2 expression and the VEGF/PAK1 signaling axis in cardiomyocytes. Once the VEGF/PAK1 pathway is upregulated, the cardiomyocytes are repaired. Our study identified a novel circRNA and illustrated the association between Pum1_0014 and miR-146a-5p, which may provide new therapeutic strategies for MI prevention and treatment.

COMPETING INTERESTS

The authors have no relevant financial or non-financial interests to disclose.

FUNDING

This study was supported by the National Natural Science Foundation of China (81960062).

AUTHORS' CONTRIBUTIONS

All authors contributed to the study's conception and design. Material preparation, data collection, and analysis were performed by Yu Tang, Yun-xia Wang, Yu-liang Zhan, Yan-feng Liu, Gui-ping Wu, and Li-dan Wen. Yu Tang wrote the first draft of the manuscript, and all authors commented on previous versions. All authors read and approved the final manuscript.

ACKNOWLEDGMENTS

Not Applicable.

ETHICS APPROVAL AND CONSENT TO PARTICIPATE

Not applicable.

CONSENT TO PUBLISH

Not applicable.

DATA AVAILABILITY

The microRNAs targeted by circRNA Pum1_0014 were predicted from StarBase (http://starbase.sysu.edu.cn/). The mRNA targeted by miR-146a-5p was predicted from TargetScan (https://www.targetscan.org/vert_80/). Other datasets generated and/or analyzed during the current study are not publicly available due to ongoing research based on the same datasets but are available from the corresponding author upon reasonable request.

REFERENCES

1. Reed GW, Rossi JE, Cannon CP. Acute myocardial infarction. *Lancet*. 2017;389(10065):197-210. doi:10.1016/S0140-6736(16)30677-8
2. Boateng S, Sanborn T. Acute myocardial infarction. *Dis Mon*. 2013;59(3):83-96. doi:10.1016/j.disamonth.2012.12.004
3. Guo X, Li Z, Vittinghoff E, Sun Y, Pletcher MJ. Trends in rate of acute myocardial infarction among patients aged <30 years. *Nat Rev Cardiol*. 2018;15(2):119. doi:10.1038/nrcardio.2017.191
4. Thum T. MicroRNA therapeutics in cardiovascular medicine. *EMBO Mol Med*. 2012;4(1):3-14. doi:10.1002/emmm.201100191
5. Samsky MD, Morrow DA, Proudfoot AG, Hochman JS, Thiele H, Rao SV. Cardiogenic Shock After Acute Myocardial Infarction: A Review. *JAMA*. 2021;326(18):1840-1850. doi:10.1001/jama.2021.18323
6. Zhang HD, Jiang LH, Sun DW, Hou JC, Ji ZL. CircRNA: a novel type of biomarker for cancer. *Breast Cancer*. 2018;25(1):1-7. doi:10.1007/s12282-017-0793-9
7. Chen LL, Yang L. Regulation of circRNA biogenesis. *RNA Biol*. 2015;12(4):381-388. doi:10.1080/15476286.2015.1020271
8. Hentze MW, Preiss T. Circular RNAs: splicing's enigma variations. *EMBO J*. 2013;32(7):923-925. doi:10.1038/emboj.2013.53
9. Bayoumi AS, Aonuma T, Teoh JP, Tang YL, Kim IM. Circular noncoding RNAs as potential therapies and circulating biomarkers for cardiovascular diseases. *Acta Pharmacol Sin*. 2018;39(7):1100-1109. doi:10.1038/aps.2017.196
10. Huang S, Li X, Zheng H, et al. Loss of Super-Enhancer-Regulated circRNA Nfix Induces Cardiac Regeneration After Myocardial Infarction in Adult Mice. *Circulation*. 2019;139(25):2857-2876. doi:10.1161/CIRCULATIONAHA.118.038361
11. Zhao B, Li G, Peng J, et al. CircMACF1 Attenuates Acute Myocardial Infarction Through miR-500b-5p-EMP1 Axis. *J Cardiovasc Transl Res*. 2021;14(1):161-172. doi:10.1007/s12265-020-09976-5
12. Si X, Zheng H, Wei G, et al. circRNA Hipk3 Induces Cardiac Regeneration after Myocardial Infarction in Mice by Binding to Notch1 and miR-133a. *Mol Ther Nucleic Acids*. 2020;21:636-655. doi:10.1016/j.omtn.2020.06.024
13. Sun W, Zhou S, Peng L, et al. CircZNF609 regulates pulmonary fibrosis via miR-145-5p/KLF4 axis and its translation function. *Cell Mol Biol Lett*. 2023;28(1):105. doi:10.1186/s11658-023-00518-w
14. Zhenhao Z, Ru C, Xiaofeng C, Heng Y, Gongxian W. A novel circular RNA, circMAML3, promotes tumor progression of prostate cancer by regulating miR-665/MAPK8IP2 axis. *Cell Death Discov*. 2023;9(1):455. doi:10.1038/s41420-023-01750-1
15. Mei X, Chen SY. Circular RNAs in cardiovascular diseases. *Pharmacol Ther*. 2022;232:107991. doi:10.1016/j.pharmthera.2021.107991
16. Schneider CA, Rasband WS, Eliceiri KW. NIH Image to ImageJ: 25 years of image analysis. *Nat Methods*. 2012;9(7):671-675. doi:10.1038/nmeth.2089
17. Larsson J, Ohishi M, Garrison B, et al. Nf2/merlin regulates hematopoietic stem cell behavior by altering microenvironmental architecture. *Cell Stem Cell*. 2008;3(2):221-227. doi:10.1016/j.stem.2008.06.005
18. Olea FD, De Lorenzi A, Cortés C, et al. Combined VEGF gene transfer and erythropoietin in ovine reperfused myocardial infarction. *Int J Cardiol*. 2013;165(2):291-298. doi:10.1016/j.ijcard.2011.08.078
19. Siede D, Rapti K, Gorska AA, et al. Identification of circular RNAs with host gene-independent expression in human model systems for cardiac differentiation and disease. *J Mol Cell Cardiol*. 2017;109:48-56. doi:10.1016/j.yjmcc.2017.06.015
20. Li X, Liu CX, Xue W, et al. Coordinated circRNA Biogenesis and Function with NF90/NF110 in Viral Infection. *Mol Cell*. 2017;67(2):214-227.e7. doi:10.1016/j.molcel.2017.05.023
21. Liu Y, Liu X, Lin C, et al. Noncoding RNAs regulate alternative splicing in Cancer. *J Exp Clin Cancer Res*. 2021;40(1):11. doi:10.1186/s13046-020-01798-2
22. Geng HH, Li R, Su YM, et al. The Circular RNA Cdr1as Promotes Myocardial Infarction by Mediating the Regulation of miR-7a on Its Target Genes Expression. *PLoS One*. 2016;11(3):e0151753. doi:10.1371/journal.pone.0151753
23. Salgado-Somoza A, Zhang L, Vausort M, Devaux Y. The circular RNA MICRA for risk stratification after myocardial infarction. *Int J Cardiol Heart Vasc*. 2017;17:33-36. doi:10.1016/j.ijcha.2017.11.001
24. Zhenzhen L, Wenting L, Jianmin Z, et al. miR-146a-5p/TXNIP axis attenuates intestinal ischemia-reperfusion injury by inhibiting autophagy via the PRKAA/mTOR signaling pathway. *Biochem Pharmacol*. 2022;197:114839. doi:10.1016/j.bcp.2021.114839
25. Zhelankin AV, Stonogina DA, Vasiliev SV, et al. Circulating Extracellular miRNA Analysis in Patients with Stable CAD and Acute Coronary Syndromes. *Biomolecules*. 2021;11(7):962. doi:10.3390/biom11070962
26. Dong M, Chen D, Zhu Y, et al. Impaired regulation of MMP2/16-MLCK3 by miR-146a-5p increased susceptibility to myocardial ischaemic injury in aging mice. *Cardiovasc Res*. 2023;119(3):786-801. doi:10.1093/cvr/cvac104
27. Ye E-A, Steinle JJ. miR-146a suppresses STAT3/VEGF pathways and reduces apoptosis through IL-6 signaling in primary human retinal microvascular endothelial cells in high glucose conditions. *Vision Res*. 2017;139:15-22. doi:10.1016/j.visres.2017.03.009
28. Zhang H, Wen H, Huang Y. MicroRNA-146a attenuates isoproterenol-induced cardiac fibrosis by inhibiting FGF2. *Exp Ther Med*. 2022;24(2):506. doi:10.3892/etm.2022.11433
29. Milano G, Biemmi V, Lazzarini E, et al. Intravenous administration of cardiac progenitor cell-derived exosomes protects against doxorubicin/trastuzumab-induced cardiac toxicity. *Cardiovasc Res*. 2020;116(2):383-392. doi:10.1093/cvr/cvz108
30. Zou J, Fei Q, Xiao H, et al. VEGF-A promotes angiogenesis after acute myocardial infarction through increasing ROS production and enhancing ER stress-mediated autophagy. *J Cell Physiol*. 2019;234(10):17690-17703. doi:10.1002/jcp.28395
31. Oduk Y, Zhu W, Kannappan R, et al. VEGF nanoparticles repair the heart after myocardial infarction. *Am J Physiol Heart Circ Physiol*. 2018;314(2):H278-H284. doi:10.1152/ajpheart.00471.2017
32. Garikipati VNS, Verma SK, Cheng Z, et al. Circular RNA CircFndc3b modulates cardiac repair after myocardial infarction via FUS/VEGF-A axis. *Nat Commun*. 2019;10(1):4317. doi:10.1038/s41467-019-11777-7